Taylor & Francis
Taylor & Francis Group

Corrosion Engineering, Science and Technology

The International Journal of Corrosion Processes and Corrosion Control

ISSN: (Print) (Online) Journal homepage: https://www.tandfonline.com/loi/ycst20

The influence of concretion on the long-term corrosion rate of steel shipwrecks in the Belgian North Sea

Kris De Baere , Sven Van Haelst , Igor Chaves , Deirdre Luyckx , Krista Van Den Bergh , Kim Verbeken , Ewoud De Meyer , Katrijn Verhasselt , Raf Meskens , Geert Potters & Rob Melchers

To cite this article: Kris De Baere , Sven Van Haelst , Igor Chaves , Deirdre Luyckx , Krista Van Den Bergh , Kim Verbeken , Ewoud De Meyer , Katrijn Verhasselt , Raf Meskens , Geert Potters & Rob Melchers (2021) The influence of concretion on the long-term corrosion rate of steel shipwrecks in the Belgian North Sea, Corrosion Engineering, Science and Technology, 56:1, 71-80, DOI: 10.1080/1478422X.2020.1807163

To link to this article: https://doi.org/10.1080/1478422X.2020.1807163

Published online: 18 Aug 2020.

CORROSION ENGINEERING, SCIENCE AND TECHNOLOGY
2021, VOL. 56, NO. 1, 71–80
https://doi.org/10.1080/1478422X.2020.1807163

The Institute of Materials, Minerals and Mining
Taylor & Francis
Taylor & Francis Group

The influence of concretion on the long-term corrosion rate of steel shipwrecks in the Belgian North Sea

Kris De Baere [a], Sven Van Haelst[b], Igor Chaves[c], Deirdre Luyckx [a], Krista Van Den Bergh [d], Kim Verbeken[e], Ewoud De Meyer[a], Katrijn Verhasselt[a], Raf Meskens[a], Geert Potters[a] and Rob Melchers[c]

[a]Antwerp Maritime Academy, Antwerp, Belgium; [b]Flanders Maritime Institute (VLIZ), Ostend, Belgium; [c]Centre for Infrastructure Performance and Reliability, University of Newcastle, Callaghan, Australia; [d]OCAS, Zelzate, Belgium; [e]Department of Materials, Textiles and Chemical Engineering, Ghent University, Ghent, Belgium

ABSTRACT

Some three hundred mainly steel shipwrecks from both World Wars lie buried at shallow depths along the Belgian North Sea coast. They were examined recently to estimate corrosion rates over periods in excess of 100 years. The rate was estimated by comparing the measured in-situ steel plate thicknesses with archived ship information. The estimates show distinctly lower long-term corrosion rate compared to that predicted by the Melchers (Modeling of marine immersion corrosion for mild and low alloy steels – part 1: phenomenological model. Corrosion. 2003;59(4):319–334) corrosion model, when parameterised for local North Sea conditions. Concretion after 50 years has a multi-layer structure for which SEM-EDS and XRD measurements show the innermost layer, close to the metal surface, consisting of akaganeite, and the outer layer mostly of calcium carbonates, silicates, and some siderite. In between there is a considerable layer of hard magnetite. The latter is proposed as the reason for the low long-term corrosion rate (0.016 mm y^{-1}) in an environment with calcium carbonate available in abundance.

ARTICLE HISTORY
Received 19 May 2020
Revised 4 August 2020
Accepted 5 August 2020

KEYWORDS
Corrosion rate; long-term corrosion model; physical–chemical processes; conservation of shipwrecks; marine infrastructures; concretion; aerobic corrosion; anaerobic corrosion; MIC

Introduction

Some three hundred mainly steel shipwrecks from both World Wars lie buried at shallow depths along the Belgian North Sea coast. Many contain the remains of their crews and therefore are protected by Belgian law. Besides their cultural and historical value, these wrecks have a biological, environmental, and economic importance. Moreover, given the detailed information available on the history of these wrecks, they are a source of information for corrosion rates over periods in excess of 100 years in a very specific environment. This is of interest since there are very few long-term data available for corrosion in actual sea conditions [1].

Marine corrosion is a major issue for infrastructure such as bridges, industrial facilities, coastal and harbour structures, pipelines especially when positioned in or near the sea. It also is an issue for offshore structures and ships. A good understanding of the corrosion processes and rates allows better estimates of the expected lifetime and reliability of such structures. It also can provide optimisation of maintenance planning, construction design (corrosion-resistant materials, acceptable corrosion rate, protective coatings, sacrificial anodes, impressed current systems, etc.) and the use of monitoring systems and tools [2]. Corrosion, particularly marine corrosion, is often considered a complicated process governed by many parameters such as temperature, water velocity, pH, dissolved oxygen, nitrate concentration, water depth, hydrostatic pressure, bacterial activity, pollutants, erosion, and surface roughness [2,3]. Most corrosion studies focus on the initial corrosion processes, leading to assessments of corrosion rates which cannot be extrapolated to longer time periods, as required for the use of marine and maritime structures, which typically have design life times of 20–30 or more years. Only a limited number of models have been proposed to describe corrosion for long-term exposures. Initial modelling efforts assumed a constant corrosion rate and showed limited consistency with reality [4]. Models already applied in the 1930s and 1940s include the well-known 'Power Model', originally proposed only empirically but later derived formally, with some mathematical approximations, by Tammann [5], originally for the atmospheric corrosion of copper roofs. Later models [6–8] proposed non-linear relations leading asymptotically to a zero-corrosion rate. Some included also the retarding effect of a protective coating, as reviewed by Melchers [4].

The present study applies the bi-modal model originally proposed by Melchers [9], largely because it is based on physical and electrochemical principles. The model is robust, is related to probabilistic principles, and can take into account uniform as well as pitting corrosion, aerobic and anaerobic conditions, as well as bacterial, environmental, and anthropogenic influences. The model consists of five phases (Figure 1). Phases 0, 1 and 2 are predominantly oxygen controlled while phases 3 and 4 are largely under anaerobic conditions. In the idealised case, the aerobic corrosion process starts with an initial instantaneous corrosion rate r_0. Owing to a progressive reduction of oxygen available at the corrosion interface the corrosion rate diminishes and becomes nearly zero, at t_a. However, the corrosion rate then increases under the influence of anaerobic and possibly bacterial corrosion processes with an initial corrosion rate of r_a to reach a constant rate r_s at time point B.

CONTACT Kris De Baere kris.de.baere@hzs.be

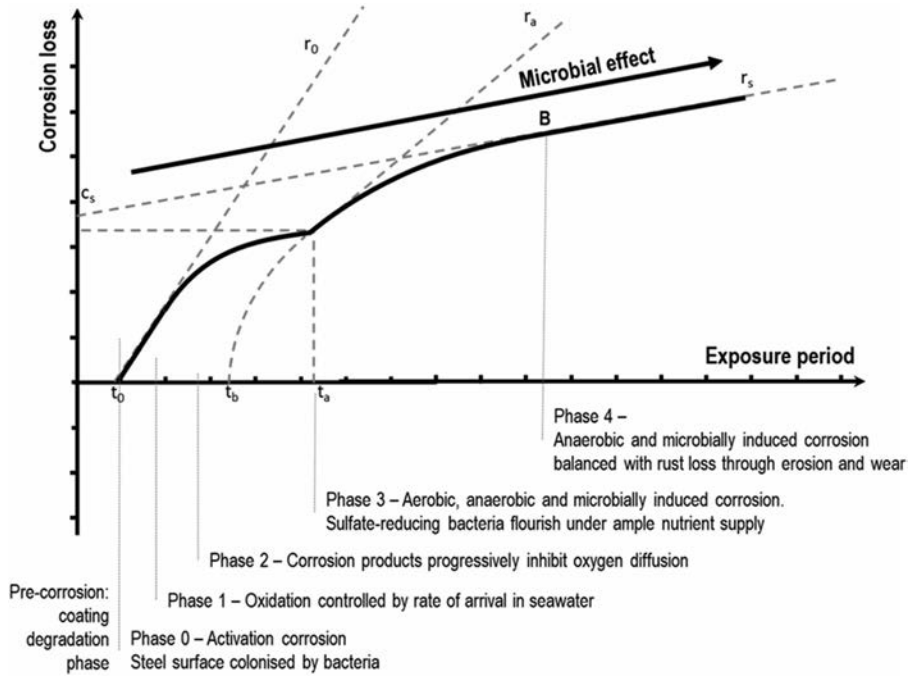

Figure 1. Multi-phase model for long-term corrosion in marine environments with indication of the parameters defined in the text and in Table 1. Long-term anaerobic corrosion rate becomes linear at $t > B$, due to a possibly increasing importance of microbiological influences over the involvement of oxygen. Figure based on Melchers [10].

The model is based on a large variety of field and relevant laboratory exposure tests, and it has been calibrated for a considerable number of environmental variables. As reviewed earlier [2], it differs considerably from all other models proposed in the literature since these are all, essentially, entirely empirical when applied to the longer-term exposure of physical infrastructure. Many of these have been applied to cases with much longer exposure periods than for which the power law was originally intended, largely because it was not incorporated that the underlying corrosion processes change from initially being aerobic at the corrosion interface to being governed eventually by the hydrogen evolution cathodic reaction [2]. Additionally, this transition does not occur for the very special case of pure copper, for which the power law was developed, but it can be seen in a variety of other metals and alloys including steels, stainless steels, aluminium, and copper alloys. Thus, simplistic curvilinear models are not appropriate, especially not when studying longer-term effects or complex materials.

At the present time it appears that the Melchers model is the best suited for long-term corrosion modelling. In addition, the model allows for longer-term exposure of interest here (i.e. well into phase 4). For the present study, this model has been parameterised using data from the Belgian North Sea shipwrecks and compared with the earlier calibration of that model. The next section describes the field investigations conducted during 2015–2019. This is followed by detailed observations and then by interpretations of the observations and proposals for further investigations.

Material and methods

Parametrisation of the Melchers model

For long-term corrosion processes, the Melchers model described in the introduction can be approximated by a linear curve with slope r_s and intercept c_s (Figure 1):

$$\text{Corrosion loss} = (c_s + [t - t_0\,] * r_s) * R_p \qquad (1)$$

where c_s is the corrosion loss back-projected to $t = 0$ (in mm) (Figure 1), t is the total time of immersion (in years), t_0 is the time to which the original coating can be considered to remain substantially protective (in years) and r_s is the anaerobic steady corrosion rate (in mm y^{-1}). R_p is a factor that can be used to model the impact of microbiologically influenced corrosion (MIC) [10]. It is a function of the concentration of dissolved inorganic nitrogen (DIN) in the local sea water environment, with

$$R_p = \frac{\text{Corrosion loss with DIN}}{\text{Corrosion loss without DIN present}} \qquad (2)$$

To parametrise R_p, DIN as well as individual concentrations of ammonia, nitrates, and nitrites in the neighbourhood of the wreck sites were derived from data available at the Flemish Marine Institute (http://www.vliz.be/en/request-data). Moreover, to apply the Melchers model to the conditions in the North Sea, the parameters graphically presented in Figure 1, were calculated according to the equations in Table 1 [2]. The temperature in the North Sea was set at an average of 12.5°C, again based on data provided by the Flemish Marine Institute. The following figure shows the geographical position of the wrecks studied (Figure 2).

Table 1. Model parameters for general corrosion and pitting under immersion conditions as a function of the average sea water temperature T, as well as applied for the North Sea ($T = 12.5$°C). Equations taken from Melchers (2005)[36].

Parameter	Unit	Equation	Value North Sea
r_0	mm y^{-1}	= 0.076·exp(0.054·T)	0.149
c_a	mm	= 0.32·exp(−0.038·T)	0.20
t_a	y	= 6.61·exp(−0.088·T)	2.20
r_a	mm y^{-1}	= 0.066·exp(0.061·T)	0.141
c_s	mm	= 0.141 − 0.00133·T	0.12
r_s	mm y^{-1}	= 0.039·exp(0.0254·T)	0.053

Figure 2. Position of the wrecks used in this study, in the Belgian Part of the North Sea and the French coast.

Corrosion measurements on shipwrecks

The Belgian part of the North Sea (BNS) [11] contains numerous shipwrecks from a variety of sources and ages (see: http://www.maritieme-archeologie.be/). Six wrecks (Table 2) were selected for the present project, based on criteria such as water depth, under water visibility, general condition and position of the wreck on the sea bottom, distance from shore, surface traffic density, location in or outside protected or restricted area, availability of dive charters and, most importantly, the availability of reliable original construction data. A seventh wreck, the submarine UC-61, in very shallow coastal water near Wissant (France) also was available. While mostly this wreck is immersed, exceptional tidal and sand displacement conditions allowed the wreck to be accessible and examined at low tide on 19 January 2019. In all cases the specific date when each ship sank is known (Table 2) allowing the duration of immersion to be determined.

The oldest wrecks in this study are three German submarines dating from the First World War. The U-11 is a German long-distance submarine that sank on 12/12/1914 after colliding with a mine. The wreck is considered to be a war grave. The UC-61 is a German minelaying submarine of the UC-

Table 2. Overview of the shipwrecks used in this study.

Name	Vessel type	Date sinking	Date measured	Source construction plans	Position	Lowest depth (m)	*n*	Original plate thickness (mm)	Average current plate thickness (mm) ± SE	Average corrosion loss per side (mm)
U-11	U-boat WWI	12/12/1914	13/5/2015	Rössler, 2002[37]	51°20,550′N 2°52,075′E	11	12	11.5	6.75 ± 0.211	2.38
U-11	U-boat WWI	12/12/1914	12/7/2019	Rössler, 2002	51°20,550′N 2°52,075′E	11	11	11.5	6.36 ± 0.602	2.57
UC-61	U-boat WWI	26/6/1917	19/1/2019	Ross, 2017[38]	50°53,552′N 1°39,79′E	0	43	11.1	7.81 ± 0.187	1.64
UB-III Fairy Bank	U-boat WWI	First half September 1918	10/2/2015	Maritime Archeology Trust, 2008	51°26,795′N 2°19,992′E	16	1	12	8.85	1.58
Torpilleur Bourrasque	Torpedo boat	30/5/1940	16/4/2019	Construction Plans – Service historique de la défense, France	51°14,964′N 2°33,026′E	16	7	8	4.54 ± 0.065	1.73
Birkenfels	Cargo ship	7/4/1966	7/2018	Construction plans	51°38,99′N 2°32,268′E	20	15	7	4.60 ± 0.175	1.20
Birkenfels	Cargo ship	7/4/1966	12/05/2015	Construction plans	51°38,99′N 2°32,268′E	20	14	7	4.70 ± 0.031	1.15
Garden City	Cargo ship	19/3/1969	10/2/2015	Construction Plans – French Lines, Le Havre, France	51°29,141′N 2°18,321′E	15	2	8	4.93 ± 0.225	1.54
Sabrina II	Fishing vessel	13/5/1972	11/5/2015	Hoekman shipbuilding, pers. comm.	51°13,300′N 2°31,121′E	15	7	7	5.14 ± 0.261	0.93

n = number of measurements taken on each ship; SE = standard error. The Birkenfels & U-11 were measured twice.

II type. She was built in 1916 and beached near Boulogne on 26 July 1917 before the crew surrendered to French authorities. The identity of the remains of the third German UB-III class submarine, situated on the Fairy Bank, is not certain. The wreck may be a submarine of the series UB-54 till UB-59 or UB-103 till UB-117. Most probably, the submarine sank after colliding with a mine in the Dover Mine Field in the first half of September 1918. The four other wrecks are shipwrecks, dating between 1940 and 1972. The Torpilleur Bourrasque is one of a series of 12 French destroyers. She was built by Ateliers et Chantiers de France at Dunkirk; she collided with a mine and was lost off Nieuwpoort on 30 May 1940 during Operation Dynamo. The Birkenfels is a German merchant vessel built in 1951. On 7 April 1966, while travelling from Bremen via Antwerp to the Persian Gulf with a cargo of 8.750 tons steel and general cargo, she collided with the German MV Marie Luise Bolton in dense fog, and sank, at about one mile south of Noordhinder Lightship. The Garden City was built at 'Le Moyne d'Iberville' in France in 1949. She sank on 19 March 1969 after a collision with a Polish vessel MV Zaglebie Dabrowskie. Finally, the Sabrina II is a Belgian trawler built in 1963, which capsized on 12 May 1972 during fishing.

Diving excursions took place between February 2015 and April 2019 and were performed by recognised scientific divers/historic wreck divers (co-author Sven Van Haelst). For the wrecks close to the shore a rigid inflatable craft (RIB) was used while for those further away the research vessel Simon Stevin of the Flanders Maritime Institute (VLIZ) was engaged. The underwater, *in situ,* plate thickness measurements were performed with a Cygnus M2-Dive equipped with the S2C single ultrasonic (UTS) Crystal Probe (Cygnus Instruments, USA) with a gauge, requiring three equally spaced echoes per spot in order to calculate a thickness measurement value.

For each of the wrecks, an easily recognisable place was selected for the measurements and for which the original plate thickness was known. Also, for all measurements in Table 2, both sides of the plate were exposed to open sea water (not buried) allowing an identical corrosion rate on front and back. A few cm^2 of the fouling and the concretion were removed with a chipping hammer and scraper used to remove loose material and to provide the UTS probe good contact, preferably direct with the metal surface, to allow measurements to be taken. In all cases these were consistent with accepted industry standards for UTS testing

Further ultrasonic measurements were taken in a similar manner at distances of about 20 cm around the first reading, resulting in n measurements per wreck (as specified in Table 2). Comparison with the original plate thickness allowed for a calculation of the corrosion rate at each individual spot.

More detailed information regarding these UTS measurement available via mail to kris.de.baere@hzs.be or sven.vanhaelst@vliz.be.

SEM-EDS and XRD analysis

On 5 August 2013, Belgium ratified the UNESCO Convention [12] on the protection of the underwater cultural heritage. This new law covers not only wrecks and wreckages but also all other forms of underwater cultural heritage both within the territorial sea and on the continental shelf. Collecting pieces of an actual wreck became morally and legally impossible. Therefore, the present study was obliged to use a work-around and instead used a piece of anchor chain not belonging to one of the shipwrecks. That piece of chain was salvaged during UXO (Unexploded Ordnance) surveys in March 2018, recovered in an area between Oostdyck and Akkaertbank at a depth of approximately 30 m and was buried approximately 50 cm in mainly sands and shells. Based on the thickness of the concretion layer (Figure 3) and the characteristics (diameter and length/width ratio) of the link [13] the chain was dated as being from the first half of the twentieth century. This corresponds closely with the age of the shipwrecks used in this study (Table 2). In turn this suggests that the steel was similar in composition and in corrosion characteristics, consistent with the literature [14,15]. Also, the chain would initially have lain on the seafloor and only gradually have become buried in the local sands, most likely well after the early corrosion products had been formed (i.e. in phases 1–3 of Figure 1). Thereafter corrosion would have been largely anaerobic, in an environment under well-developed rusts and thus largely independent of the external environment. Importantly, sea water and by implication dissolved oxygen and calcareous material are likely to have been present almost as much as if the links had been on the surface instead of shallow burial. From this it was concluded that examination of the chain links was an adequate surrogate for examination of the rusts on the wrecks.

In a first series of measurements, X-ray diffraction (XRD) was used to determine a preliminary composition of the concretion around the metal chain shackle a D8 Discover XRD (Bruker), set-up for phase identification with a Co tube ($K\alpha 1 = 1.78897$ Å) with a generator at 35 kV and 40 mA, a 1 mm slit behind the Polycap, long soller slits 0.35° in front of the detector, the lynx eye detector in 0 D mode with an opening of 13 mm, and a q/q configuration (continuous locked couple scan). The crystalline phases present in the analysed sample were identified by comparing the positions of diffraction peaks in the experimental pattern with those present in (experimental and simulated) patterns of known samples available in a database (Powder Diffraction File, International Centre for Diffraction Data, Swarthmore/USA).

Next, the chain was cut into pieces of approximately 5 cm. One of the pieces was forwarded to the University of Newcastle in Australia for detailed analysis. Upon reception, the sample was stored in a dry and secure location under ambient conditions for about 6 weeks prior to testing. The chain pieces

Figure 3. Piece of historic chain used for SEM-EDX and XRD analysis of the concretion layers.

were dried in an oven at 110°C for 24 h prior to SEM/EDS and XRD testing. Target areas of interest were marked and aligned in the PANalytical X'Pert Pro MRD XRD for analysis, which was used with a continuous scan type, step time of 135 s, at 25°C using a Cu anode with beam generator set to 40 mA, 40 kV.

To prepare the sample for Zeiss SIGMA VP SEM/EDS analysis, the chain was ground flat using a 400 grit silica carbide belt sander and then broken open to obtain suitable samples for Scanning Electron Spectroscopy (SEM) with Electron Dispersive Spectroscopy (EDS) analysis. The Back Scatter Electron Detector was used for observation when necessary, while the analysis was primary completed using the Secondary Electron Detector at a 20 keV beam intensity. When performing EDS scans, all zones had the same magnification and the scan was performed for the same duration; sufficient time was allowed (approx. 10 min) until no further changes to peak count were detectable.

Results and discussion

Model parametrisation

The Melchers model was parametrised for the North Sea, with parameter values as estimated and presented in Figure 1 based on the equations in Table 1. As most of the wrecks of interest have been immersed for a very long time (>15 years), the linear approximation of the Melchers model (Equation (1)) is appropriate. The value for R_p in this equation can be determined with an empirical relation between R_p and the concentration of DIN (dissolved inorganic nitrogen) for long term exposures [10]:

$$R_p = 1.375 \cdot \mathrm{DIN} + 1 \tag{3}$$

with DIN expressed in mg N L^{-1}. Values for DIN measured in the North Sea vary between 0.3 mg N L^{-1} [16] and 1.4 mg N L^{-1} [17], which are comparable with previously published average values of 0-30 µM (0–0.4 mg N L^{-1}) nitrate, 0–2 µM (0.03 mg L^{-1}) nitrite and 0–25 µM (0-0.35 mg N L^{-1}) ammonia for unpolluted coastal waters [18].

Melchers [10] obtained a strong relationship between the availability of DIN for microbiological activity and the severity of the resulting MIC, noting that the DIN in the water is only a proxy for MIC. This is the case also for the waters surrounding the wrecks. Since sulfate reducing bacteria (SRB) usually are considered the most common corrosion-accelerating bacteria, attention was given to estimating their presence. They are known to produce sulphides, mainly in the form of iron sulphides, in their main energy metabolism, and this can be used as a marker for their presence. In this context, it is noted that earlier XRD analysis in 2019 of a piece of an iron chain conserved under the same conditions as the shipwrecks failed to demonstrate the presence of iron sulphides [19]. That sample did contain SiO_2, $CaCO_3$, $K_2CaMg(SO_4)_3$, FeOOH, K_3FeO_2, $Fe_{0.94}O$, $CaFeO_3$ and $Fe_8O_8(OH)_8Cl$. For the present study DNA sampling was attempted on a sample taken from within the concretion layer around the iron chain shackle. The extraction yielded very low DNA concentrations. The subsequent PCR of 16S rRNA genes did not result in any amplification of the genetic material. This is probably due to very low amounts of bacteria, and presumably nutrients, within the concretion layer. How this relates to the elevated DIN conditions outside the concretion layer, that is, within the local sea water, remains an interesting question. In this context it is noted there could be the presence of inhibitory compounds in the North Sea sea water [16]. Overall, these results suggest that MIC may be insignificant for the corrosion of the shipwrecks considered here. The factor R_p can therefore be kept at a value of 1. Hence, according to the Melchers model (Table 1) the long-term corrosion rate, that is after a period of approximately 15 years on the sea bottom at 12.5°C, is predicted to be r_s, = 0.053 mm y^{-1}.

Estimation of shipwreck corrosion rate

To make an estimate of the long-term corrosion rate r_s specifically for the Belgian North Sea wrecks, the results of the average measured corrosion losses on the shipwrecks were plotted against the period of immersion. The empirically obtained trend (Figure 4) was compared with the multi-phase model of Melchers at 12.5°C in the absence of MIC [2].

For the predominantly anaerobic part of the model (phases 3 and 4), there is a steep increase in corrosion loss, starting for phase 3, at t_a, followed eventually by a linear function (phase 4). The exact value of t_a depends mainly on water temperature but cannot be estimated from the data at hand, as all considered shipwrecks have been immersed for many years; the minimum being 43 years (Sabrina II). In all cases, it is likely that the vessels were coated, and the likely life of such coatings needs to be considered. This has never been studied in any detail for shipwrecks. Even estimating the durability of modern coatings poses significant problems. A survey by Verstraelen et al. [20] suggests that, on average, ballast tank coatings remain sufficiently intact for a period of 10 years. Another survey suggests coating breakdown occurs much earlier and that 10 years is consistent with complete coating breakdown for plates but with a range of ±3 years around the mean, and larger scatter for edges and welds [21]. Calculations based on the equations given in Table 1 give a time interval between t_0 and t_a of approximately 2.2 years, so that t_a = 12.3 years (taking into account a coating life of 10.1 years) is considered reasonable. This was allowed in fitting the trend to the data. It could be approximated by the power law as follows:

$$\text{Corrosion loss} = \alpha.(t - t_b)^{\beta}, \tag{4}$$

where $t_b = 12$ years, $\alpha = 0.15$ (95% confidence interval [0.036 ; 0.65]) and $\beta = 0.57$ (95% confidence interval [0.122 ; 0.93]). This model is statistically significant (p = 0.006 < 0.05). For this model, t_a is reached at 12.3 years after sinking, when the tangent to the model has a slope of $r_a = 0.141$, based on the equations in Table 1.

A long-term linear model was also fitted on the data (Equation (5)). As can be seen in Figure 4, the long-term evolution of average corrosion loss differs little between the linear and the non-linear trends. The linear model was therefore adopted:

$$\text{Corrosion loss} = c_s + t{*}r_s \tag{5}$$

Equation (5) is essentially the same as Equation (1), except that in Equation (5), time t is the period (years) after sinking. The long-term corrosion rate is estimated at $r_s = 0.016$ mm y^{-1} (95% confidence interval [0.0053 ; 0.0268]), while the intercept is given by $c_s = 0.43$ (95% confidence interval

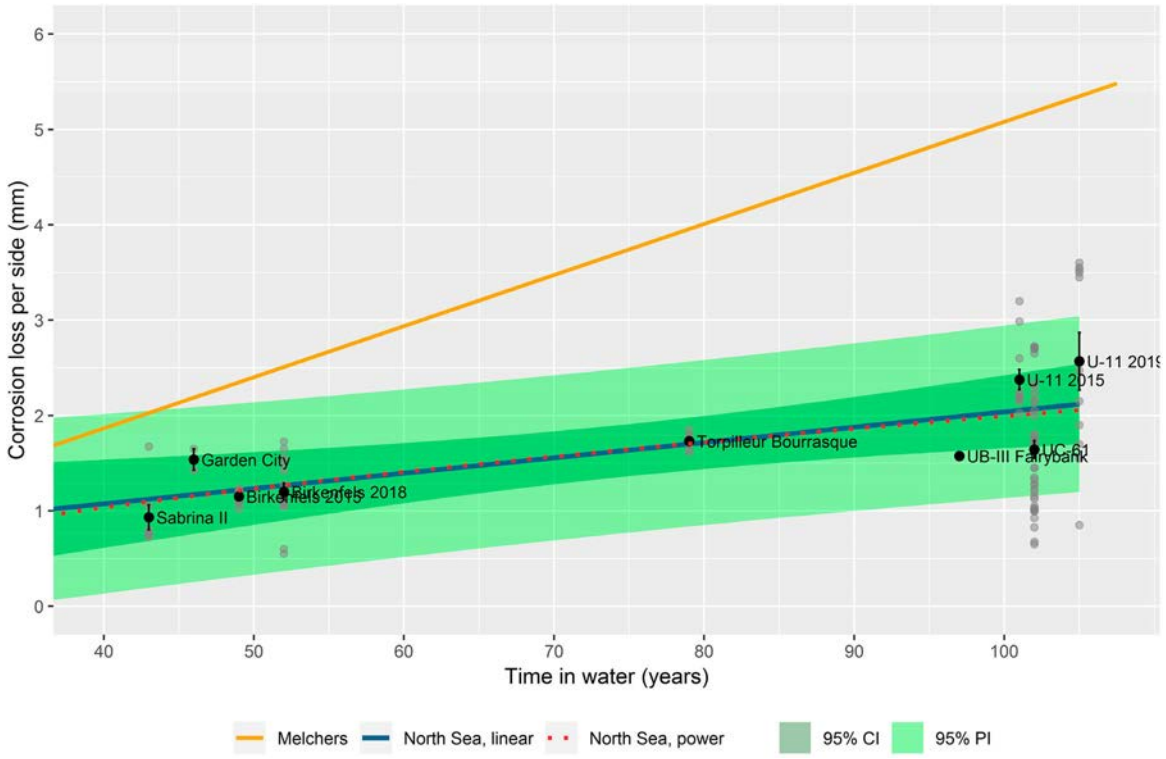

Figure 4. Corrosion loss per side (mm) versus time in the water in years; the blue line corresponds with the linear North Sea model with a green 95% confidence and prediction band; the orange line corresponds with the Melchers model as parametrised for the North Sea; the red dotted line corresponds with the North Sea power model.

[−0.42 ; 1.28]). This model is statistically significant ($p = 0.009 < 0.05$).

A comparison of the long-term linear model (displayed along with its 95% confidence and prediction bands in Figure 4) with the linear stage 4 of Melchers model (as defined in Figure 1) shows that the linear part of the latter has a much higher long-term corrosion rate. The corrosion rate for the ship wrecks considered, all located in the Belgian part of the North Sea (BNS), is less than one-third of the corrosion rate predicted by Melchers' multi-phase model ($r_s = 0.054$ mm y^{-1}) (Table 1).

Although it is sometimes claimed that it is difficult to generalise corrosion rates of iron and steel in sea water [22], it should be remembered that the Melchers model was based on a very large data set, including other data in the North Sea (near Scotland) [9]. Because of the non-linearity displayed in the bi-model model for corrosion simple comparisons of corrosion rates without allowing for the early part of the model can give quite misleading interpretations. This can be seen by consideration of data reported by others. For example, field corrosion rate tests in shallow water (28 m) and in the deep sea (2511 m) in the Sea of Japan obtained corrosion rates in deep water of 0.055 mm y^{-1} after (only) 1.4 y, decreasing to 0.035 mm y^{-1} after 8.6 y [23]. In shallow water they obtained a rate of 0.229 mm y^{-1} after 124 days. Macleod [24] reported a corrosion rate of 0.095 mm y^{-1} on the wreck of the Yubae Maru, found in Chuuk lagoon at a depth of 28 m. These rates are all considerably larger than the long-term rate in the Belgian North Sea, but do not account for the variation with time as indicated by the model.

The present findings suggest that it is necessary to investigate more fully the characteristics of corrosion specifically in the Belgian part of the North Sea and perhaps other locations that have similar local conditions. To throw some light on what might be different about steel corrosion in the Belgian part of the North Sea, the next sections report detailed observations of the rusts on the wrecks and similar objects in this part of the North Sea.

Analysis of corrosion product layers

SEM/EDS analysis

One of the features seen on the corroded wrecks (and other steel objects) in the Belgian part of the North Sea is the heavy coverage with calcareous deposits (concretion layer). These have been observed in some other immersion corrosion, particularly off Western Australia [25] and some sites in the US [26] but overall are not common for marine corrosion. To obtain some understanding of the characteristics of the concretion layers, several distinct parts of steel chain link available for analysis (see above) were selected, based on their position relative to the metal surface and their difference in colour (Figure 5). This shows that there is a substantial amount of calcium ions in the outer, whitish-coloured, corrosion product. The layers closer to the original steel are high in Fe as expected.

XRD analysis

For the XRD analyses, six distinct zones were considered of interest, starting at the metal structure, and then outward towards the outer surface of the concretion (see Figure 6). Two locations (A and B) were chosen directly near the steel chain surface and inside the concretion, assumed representative of the direct corrosion products. At both locations, the products consist almost entirely of akaganeite (β-FeOOH). On the exterior surface, at location F (taken at the outer layers

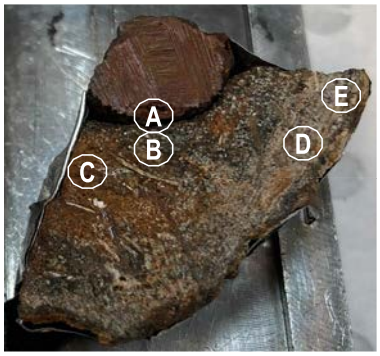

Indicative % volume

From chain to outer surface

Element / Zone	Si (varies)	Fe (decrease)	Mg (same)	S (same)	Ca (increase)	Cl (decrease)
A (steel)	0.2	5.5	Trace	0.5	Trace	1.4
B (interface)	9.2	0.7	0.3	0.4	1.1	0.6
C (Brown)	1.4	1.0	0.4	0.9	1.8	0.3
D (White)	0.8	Trace	0.9	0.5	10.0	Trace
E (White)	4.8	0.2	0.4	0.4	7.0	Trace

Figure 5. SEM/EDS analysis of five locations ranging from the metal surface towards the outer layers of the concretion. The values in table are expressed in atomic weight %.

of the accretion) and E (taken in between two parts of the chain link), deposits of calcium and magnesium minerals were noted, mixed with silica oxides and silicates with mineral structures of quartz (SiO_2), tilleyite ($Ca_5Si_2O_7(CO_3)_2$), dolomite ($CaMg(CO_3)_2$) and gypsum ($CaSO_4$), next to large amounts of calcite and aragonite (forms of $CaCO_3$) 17% and 57% at location 1, respectively, and for 10% and 36% at location 3. Both locations also contained 8% and 6% of siderite, respectively. At locations C and D, black and orange rusts were found. These rusts were akaganeite (46% and 32%), mixed with goethite (12% and 17%) and magnetite (19% and 11%). Some quartz and gypsum were also observed. Table 3 summarises the results. For comparison, some results are shown also for long-term rust developed on ferrous objects buried in coastal region soils some 100 km southwest of the Belgian North Sea coast [27]. This comparison is made because at this site the corrosion products also were found to have calcite and aragonite contents, unlike what is conventionally found in rust products for buried ferrous objects [28]. It is noted that the components of the rust products in soil environment show similarities with those from sea water immersion, particularly the presence of the chloride-bearing akaganeite. This suggests a degree of correspondence in corrosion mechanisms between these two environments that might be further investigated, noting that classical literature has very little to say about corrosion in calcareous soils [28].

Discussion

The present investigation used observations on a number of shipwrecks with ages extending over a considerable period. It would be expected that the wrought irons and steels used for the construction of the ship hulls varied in composition. However, due to archaeological reasons, this could not be investigated. While there could be a small effect of steel composition on long-term corrosion, there is enough evidence in the literature that any such effect is small, both for shorter-term exposures and for longer-term [14,15]. This means that the difference between the long-term rate from the Melchers model and that observed in the Belgian part of the North Sea (BNS) cannot be explained in terms of steel (or wrought iron) composition.

The formation of a concretion layer on the surface of metal objects, such as described above, and as observed in the present cases, is known to initiate relatively soon, i.e. within months, after first immersion [22,26,29–31]. This concretion layer, initially [30] largely calcium carbonate, has been noted to become relatively impermeable to oxygen with increased exposure period, largely due to the formation of ferrous carbonate ($FeCO_3$) and thereby tending to slow down the corrosion rate, at least for shorter periods of exposure [26,32]. The SEM-EDS and XRD measurements presented herein show that calcium carbonate also resides within the rust layers, and that $FeCO_3$ also likely occurs there, consistent with earlier observations [26].

It is well-known that soon after first immersion of iron or steel in sea water the initial corrosion products are various iron hydroxides and that these are associated with elevated pH at the metal surface [26,27,33]. These regions are preferential for the deposition of any calcium carbonate precipitation in sea waters with a larger tendency for calcium carbonate to come out of solution, and to do so for long periods of time – i.e. throughout the exposure period.

Importantly, calcareous deposition observed in the present investigation and in some others is not universal. It does not occur, for example, in the northern part of the North Sea [34]. This indicates that there are very particular conditions in the BNS that tend to favour calcareous deposition. These are unlikely to be short-term effects such as caused by anthropological influences, since the shipwrecks are in some cases over 100 years old and water pollution in the North Sea has changed very considerably over that time [16]. One clue for the high calcareous deposition and the slower rates of corrosion rate lies in the presence of a number of limestone sands and geological formations in the region of the BNS, for example, the white cliffs of Dover. There is evidence that the BNS region and the sea water itself in this region is a significant repository of calcareous material. For example, Zintzen et al. [35], from an inventory of the epifauna of the shipwrecks Birkenfels and Bourrasque, noted that most organisms had calcium skeletons or exoskeleton. It is feasible that these could contribute to the formation of the outer calcium layers on any corroding object [30] and also to the calcareous content within the rust layers. Again, the precise mechanisms involved remain for further investigation.

Regarding the distribution of the different corrosion products and the carbonates through the rust layers (Table 3), it is noted that this is consistent with the observations reported by Neff et al. [27] for calcareous soils, noting that these had low chloride contents. The present observations also are largely consistent with those of North & MacLeod [30] for corrosion in sea waters off the Western Australian coast. Despite these consistencies, it is clear that improved explanations are required to fully account for the

Figure 6. XRD results Belgian North Sea chain link. 6 zones were distinguished from A to F. A is the closest to the remaining metal of the chain and F is the accretion edge. The XRD results are shown in % volume (indicative)

Table 3. Identification of the different corrosion layers around the Belgian North Sea chain link, compared to the model proposed by Neff et al. [27].

	Main components (Figure 6)	Corrosion layers[a] observed by Neff et al. [27]
Calcium concretion	Zone E and F: Quartz Calcite and aragonite Siderite	TM (Transformed Medium): $CaCO_3$, SiO_2, $NaAlSi_3O_3$, $FeCO_3$
Magnetite	Zone C and D: Akaganeite Magnetite Quartz and gypsum	DPL (Dense product Layer): Fe_3O_4, β-FeOOH($Cl_{0.19}$)
Corrosion products	Zone A and B: Akaganeite	
Steel structure of original artefact M (Metal)		

[a]For ferrous objects buried in coastal, chloride-bearing soils near the coast.

development of a steady state corrosion rate in highly calcareous sea waters, from first immersion to eventual long-term corrosion with the effect of calcium carbonate deposition within and on the external surfaces of the rust layers. That explanation should also allow for a range of calcium carbonate conditions, noting that corrosion products do not always show evidence of calcareous products either within or on the surface of the rusts.

Conclusion

The investigation of seven steel and wrought-iron shipwrecks buried in shallow depths along the Belgian North Sea with some exposed for more than 100 years produced the following results:

(1) The long-term corrosion rate corresponding to phase 4 in the bi-modal model (2003) was found to be 0.016 mm y^{-1} with a precision (SE) of 0.0045, a rate much lower than predicted by the bi-modal model even though that was based on an extensive set of world-wide data,
(2) Field observations showed that there was extensive calcareous deposition on the outside surfaces of the rusts and SEM-EDS and XRD observations showed that besides the usual presence of magnetite within the rust layers there were also calcium and ferrous carbonates,
(3) The calcium and ferrous carbonates within the rust layers were found to be very dense and hard indicating a low degree of permeability for diffusion of oxygen and other ions, thereby reducing the rate of long-term corrosion,
(4) The high degree of calcareous deposition in the Belgian part of the North Sea where the shipwrecks are located is consistent with local observations of an unusually high presence of invertebrate fauna with calcium-based exoskeletons,
(5) The low long-term corrosion rate may have consequences for future conservation techniques and policies, including calculation of associated longevity and risk, as well as cost benefit decisions for prioritising management actions and the best use of budgets.

Acknowledgements

This project was partially funded by the DISARM SBO project funded by the National Science Fund in Flanders, Belgium, as well as by the Internal Projects 'Modellering van corrosie van de omhulsels van de giftige munitie op de Paardenmarkt' (Modelling the condition of the poisonous ammunition on the Paardenmarkt)' and 'Conservatie van historische Noordzeewrakken (Conservation of historical North Sea wrecks)' at the Antwerp Maritime Academy. The authors thank Yves Van Ingelghem (Free University of Brussels) for his contributions to the technical discussions. Klaas Hoekman of Hoekman shipbuilding provided the construction details of the Sabrina II. All of the diving expeditions would have been impossible without the support of the Flanders Marine Institute. The authors also would like to acknowledge use of the facilities and technical assistance of Jenny Zobec and Yun Lin EMX Laboratory staff members of the University of Newcastle Australia.

Disclosure statement

No potential conflict of interest was reported by the author(s).

Funding

This project was partially funded by the DISARM SBO project funded by the National Science Fund in Flanders, Belgium, as well as by the Internal Projects 'Modellering van corrosie van de omhulsels van de giftige munitie op de Paardenmarkt' (Modelling the condition of the poisonous ammunition on the Paardenmarkt)' and 'Conservatie van historische Noordzeewrakken (Conservation of historical North Sea wrecks)' at the Antwerp Maritime Academy.

ORCID

Kris De Baere http://orcid.org/0000-0002-3461-3521
Deirdre Luyckx http://orcid.org/0000-0003-2308-8060
Krista Van Den Bergh http://orcid.org/0000-0001-7475-7901

References

[1] Moore JD. Long-term corrosion processes of iron and steel shipwrecks in the marine environment: a review of current knowledge. J Maritime Archaeol. 2015;10:191–204.
[2] Melchers R. Progress in developing realistic corrosion models. Struct Infrastruct Eng. 2018;14:843–853. doi.org/10.1080/15732479.2018.1436570.
[3] Roberge PR. Handbook of corrosion engineering. New York (NY): McGraw Hill Handbooks; 2000.
[4] Melchers R. Predicting long-term corrosion of metal alloys in physical infrastructure 3, Article number: 4. Opgehaald van Materials Degradation, 2019 Jan. DOI:10.1038/s41529-018-0066-x.
[5] Tammann G. Lehrbuch der metallographie: chemie und physik der metalle und ihrer legierungen. Leipzig: Voss; 1923.
[6] Paik J, Kim S, Lee S, et al. A probabilistic corrosion rate estimation model for longitudinal strength members of bulk carriers. J Ship Ocean Technol. 1998;2:58–70.
[7] Qin S, Cui W. Effect of corrosion models on the time-dependent reliability of steel plated elements. *Marine* Struct. 2002;15:15–34.
[8] Guedes-Soares C, Garatov Y, Zayed A, et al. Non-linear corrosion model for immersed steel plates accounting for environmental factors. Trans Soc Nav Archit Ma. Eng. 2006;113:306–329.
[9] Melchers R. Modeling of marine immersion corrosion for mild and low alloy steels – part 1: phenomenological model. Corrosion. 2003;59(4):319–334.
[10] Melchers R. Long-term immersion corrosion of steels in seawaters with elevated nutrient concentration. Corros Sci. 2014;81:110–116.
[11] Lescrauwaet A, Pirlet H, Verleye T, et al. Compendium Voor Kust En Zee: Een Geïntegreerd Kennisdocument Over De Socio-economische, Ecologische En Institutionele Aspecten Van De Kust En Zee In Vlaanderen En België. Oostende: VLIZ – Vlaams Instituut Voor De Zee; 2013.
[12] Archeologisch erfgoed in de Noordzee. Opgehaald van SeArch Eindconferentie, verdronken erfgoed, sd. Available from: http://www.vliz.be/projects/sea-arch/index.htm.
[13] Johnson D, Medlin D, Murphy L, et al. In corrosion rate trajectories of concreted iron and steel shipwrecks and structures in seawater – the Weins number. Corrosion. 2011;67(12):125005-1–125005-9.
[14] Evans U. The corrosion and oxidation of metals: scientific principles and practical applications. London: Edward Arnold; 1960.

[15] Melchers R. Effect of small compositional changes on marine immersion corrosion of low alloy steel. Corros Sci. 2004;46 (7):1669–1691.
[16] OSPAR. Eutrophication status of the OSPAR maritime area – third integrated report on the eutrophication status of the. OSPAR; 2017.
[17] Janssen G. De eutrofiëring van de Noordzee en Waddenzee, een tussenbalans. Zien we al resultaten van het saneringsbeleid. H2O. 1993;26(4):86–91.
[18] Sharp J. The distribution of inorganic nitrogen and dissolved and particulate organic nitrogen in the seaNitrogen in the marine environment Vol. Chapter 1. New York, USA: Academic Press; 1983. p. 1–35.
[19] De Baere K, Melchers R, Van Haelst S, et al. Corrosion of steel and other wreckage in the Belgian North Sea. (p. paper 076). Melbourne – 24 till 27 November 2019: ACA.
[20] Verstraelen H, De Baere K, Schillemans W, et al. In situ study of ballast tank corrosion on ships (part 2). Mater Perform. 2009;48 (11):54–57.
[21] Melchers R, Jiang X. Estimation of models for durability of epoxy coatings in water ballast tanks. Ships Offsh Struct. 2006;1(1):61–70.
[22] Memet J. The corrosion of metallic artefacts in seawater: descriptive analysis. In: Dillmann P, Béranger G, Piccardo P, Matthiesen H, editors. Corrosion of metallic heritage artefacts. Cambridge: Woodhead Publishing; 2007. p 152–169.
[23] Kuroda T, Takai R, Kobayashi Y, et al. Corrosion rate of shipwreck structural steels under the seaOceans 2008. Kobe, Japan: MTS/IEEE Kobe Techno-Ocean; 2008. p. 1–610.1109/OCEANSKOBE.2008.4531052.
[24] Macleod I. In-situ corrosion measurements of WWII shipwrecks in Chuuk lagoon, quantification of decay mechanisms and rates of deterioration. Front Marine Sci. 2016;3(art. 38):1–10.
[25] MacLeod I. Corrosion and conservation management of iron shipwrecks in Chuuk lagoon, federated states of Micronesia. Conserv Manage Archaeol Sites. 2006;7:203–223.
[26] LaQue F. Marine corrosion: causes and prevention (The corrosion monograph series). La Jolla (CaliforniaUSA: Wiley; 1975ISBN: 0-471-51745-3.
[27] Neff N, Dillman P, Bellot-Gurlet L, et al. Corrosion of archeological artefacts in soil: characterisation of the corrosion system. Corros Sci. 2005;47:515–535.
[28] Romanoff M. Underground corrosion – circular 579. Washington (DC): US Government Printing Office; 1957.
[29] North N. Formation of coral concretion on marine iron. Int J Naut Archeol Underw Explor. 1976;5:253–258.
[30] North N, MacLeod I. Corrosion of metals. In: Pearson C, editor. Conservation of marine archaeological objectsElsevier; 1988. p. 68–98doi.org/10.1016/C2009-0-24193-6.
[31] McCarthy M. Site formation processes. In: Iron and steamship archaeology. Kluwer; 2002. p. 91–93.
[32] Green G. Maritime archeology, a technical handbook. 2nd ed. New York (NY) Taylor & Francis; 2016.
[33] Butler G, Stretton P, Beynon J. Initiation and growth of pits on high-purity iron and its alloys with chromium and copper in neutral chloride solutions. Br Corros J. 1972;7:168–173.
[34] Blekkenhorst F, Ferrari G, van der Wekken C, et al. Development of high strength low alloy steels for marine applications, part 1: results of long term exposure tests on commercially available steels. Br Corros J. 1986;21(3):163–176.
[35] Zintzen V, Massin C, Norro A, et al. Epifaunal inventory of two shipwrecks from the Belgian continental shelf. Hydrobiologia. 2006;555:207–219.
[36] Melchers Robert E., Jeffrey Robert. Early corrosion of mild steel in seawater. Corrosion Science. 2005;47(7):1678–1693. 10.1016/j.corsci.2004.08.006
[37] Rössler Eberhard. The U-Boat: The Evolution and Technical History of German Submarines . London, UK: Cassell ; 2002ISBN-13: 978-0304361205
[38] Ross David. Submarines: WWI to the present. London, UK: Chartwell Books; 2017ISBN-13: 978-0785834465